Tyrosine Phosphorylation of Caveolin-2 at Residue 27: Differences in the Spatial and Temporal Behavior of Phospho-Cav-2 (pY19 and pY27)†

Xiao Bo Wang,‡ Hyangkyu Lee,‡,§ Franco Capozza,‡ Shana Marmon,‡ Federica Sotgia,‡ James W. Brooks,|| Roberto Campos-Gonzalez,|| and Michael P. Lisanti*,‡

Department of Molecular Pharmacology and the Albert Einstein Cancer Center, Albert Einstein College of Medicine, 1300 Morris Park Avenue, Bronx, New York 10461, Program in Epithelial Biology, Stanford University School of Medicine, 269 Campus Drive, Stanford, California 94305, and Department of Cell Signaling Research, BD Biosciences, 11077 North Torrey Pines Road, La Jolla, California 92037

Received April 8, 2004; Revised Manuscript Received July 1, 2004

ABSTRACT: Caveolin-2 is an accessory molecule and the binding partner of caveolin-1. Previously, we showed that c-Src expression leads to the tyrosine phosphorylation of Cav-2 at position 19. To further investigate the tyrosine phosphorylation of Cav-2, we have now generated a novel phospho-specific antibody directed against phospho-Cav-2 (pY27). Here, we show that Cav-2 is phosphorylated at both tyrosines 19 and 27. We reconstituted this phosphorylation event by recombinantly coexpressing c-Src and Cav-2. We generated a series of Cav-2 constructs harboring the mutation of each tyrosine to alanine, singly or in combination, i.e., Cav-2 Y19A, Y27A, and Y19A/Y27A. Recombinant expression of these mutants in Cos-7 cells demonstrated that neither tyrosine is the unique phosphorylation site, and that double mutation of tyrosines 19 and 27 to alanine abrogates Cav-2 tyrosine phosphorylation. Immunofluorescence analysis of NIH 3T3 cells revealed that the two tyrosine-phosphorylated forms of Cav-2 exhibited some distinct properties. Phospho-Cav-2 (pY19) is concentrated at cell edges and at cell−cell contacts, whereas phospho-Cav-2 (pY27) is distributed in a dotlike pattern throughout the cell surface and cytoplasm. Further functional analysis revealed that tyrosine phosphorylation of Cav-2 has no effect on its targeting to lipid rafts, but clearly disrupts the hetero-oligomerization of Cav-2 with Cav-1. In an attempt to identify upstream mediators, we investigated Cav-2 tyrosine phosphorylation in an endogenous setting. We found that in A431 cells, EGF stimulation is sufficient to induce Cav-2 phosphorylation at tyrosines 19 and 27. However, the behavior of the two phosphorylated forms of Cav-2 diverges upon EGF stimulation. First, phospho-Cav-2 (pY19) and phospho-Cav-2 (pY27) display different localization patterns. In addition, the temporal response to EGF stimulation appears to be different. Cav-2 is phosphorylated at tyrosine 19 in a rapid and transient fashion, whereas phosphorylation at tyrosine 27 is sustained over time. Three SH2 domain-containing proteins, c-Src, Nck, and Ras-GAP, were found to associate with Cav-2 in a phosphorylation-dependent manner. However, phosphorylation at tyrosine 27 appears to be more critical than phosphorylation at tyrosine 19 for this binding to occur. Taken together, these results suggest that, in addition to the common characteristics that these two sites appear to share, phospho-Cav-2 (pY19) and phospho-Cav-2 (pY27) may each possess a set of unique functional roles.

Caveolae are 50−100 nm plasma membrane invaginations, which are found in a variety of cell types, and are particularly abundant in fibroblasts, adipocytes, epithelial cells, endothelial cells, type I pneumocytes, and muscle cells (*1*−*3*). Although the precise role of this organelle has remained obscure for many years, more recently many attempts have been undertaken to clarify the physiological functions of caveolae within the cell.

Caveolae are thought to be involved in many different processes, including vesicular transport, cellular cholesterol homeostasis, and signal transduction (*4*−*8*). Studies on cellular and mouse models have now conclusively shown that the structural components of caveolae organelles are proteins belonging to the caveolin family. The three members of this family, caveolin-1, -2, and -3, present different tissue distributions, with caveolin-1 (Cav-1)[1] and caveolin-2 (Cav-2) being coexpressed in fibroblasts, epithelial cells, adipocytes, endothelial cells, and type I pneumocytes (*9*−*11*), whereas caveolin-3 (Cav-3) expression is restricted to muscle cells (*12*−*14*). Sequence alignments show a high degree of homology between Cav-1 and Cav-3 and between Cav-1 and Cav-2.

† This work was supported by grants from the National Institutes of Health (NIH) and the Susan G. Komen Breast Cancer Foundation, as well as a Hirschl/Weil-Caulier Career Scientist Award (all to M.P.L.). X.B.W. and H.L. were supported by an NIH Graduate Training Program Grant (T32-DK07513). S.M. was supported by a National Institutes of Health Medical Scientist Training Grant (T32-GM07288).

* To whom correspondence should be addressed. Telephone: (718) 430-8828. Fax: (718) 430-8830. E-mail: lisanti@aecom.yu.edu.

‡ Albert Einstein College of Medicine.

§ Stanford University School of Medicine.

|| BD Biosciences.

[1] Abbreviations: Cav-1, caveolin-1; Cav-2, caveolin-2; Cav-3, caveolin-3; EGF, epidermal growth factor; IPTG, isopropyl 1-thio-β-D-galactopyranoside; MAP, mitogen-activated protein.

10.1021/bi049295+ CCC: $27.50
Published on Web 10/08/2004

Caveolins are essential for caveolar biogenesis and function (*15, 16*). Depending on the cell type, Cav-1 or Cav-3 expression is the *sine qua non* for the formation of caveolae membranes *in vivo* (*17*−*19*). However, normal caveolae continue to be found in the absence of Cav-2 expression (*20*), suggesting that Cav-2 might play a more regulatory role in caveolae formation. In support of this idea, recent studies have shown that phosphorylation of Cav-2 on serine 23 and 36 regulates Cav-1-dependent caveolae formation (*21*).

Certain physical and biochemical properties of caveolins, for example, the abilities to oligomerize (*22*) and to bind cholesterol (*23*), constitute focal points in the formation of caveolae. Cav-1 and Cav-3 can form homotypic high-molecular mass oligomers containing ~14−16 molecules (*12, 22, 24*), whereas Cav-2 can only form heterotypic oligomers with Cav-1 (*25*). During their synthesis, at the level of the endoplasmic reticulum, Cav-1 associates with Cav-2 and forms a hetero-oligomeric complex (*22, 24, 26*). As a result of Cav-1's ability to bind cholesterol, this complex is then inserted into membrane microdomains that are highly enriched in cholesterol and sphingolipids, termed lipid rafts (*27*). In the Golgi complex, adjacent caveolin oligomers undergo a second oligomerization stage, which ultimately drives the formation of a caveolae-sized vesicle (*28, 29*). In the absence of Cav-1, Cav-2 forms a mixture of monomers and dimers, which are not able to exit the Golgi, and are subsequently degraded by the proteasomal machinery (*17, 30, 31*).

It is now widely accepted that caveolae play an important role in compartmentalizing and modulating a variety of signal transduction processes. A number of signaling-related molecules, including receptor and nonreceptor tyrosine kinases, G-protein-coupled receptors, ion channels, adaptor proteins, and structural proteins, are specifically localized within caveolae (*32*−*34*). Many of the molecules, which are targeted to caveolae membranes, contain lipid modifications. Well-characterized caveolae-associated proteins such as Src-family tyrosine kinases, H-Ras, heterotrimeric G-protein α subunits, and endothelial nitric oxide synthase (eNOS) all carry one or more myristoyl, palmitoyl, or fatty acyl groups (*35*−*38*).

Cav-1 was first identified as one of the major tyrosine-phosphorylated proteins in chicken embryo fibroblasts transformed by the v-Src oncogene (*39*). We have previously shown that tyrosine 14 is the principal site for c-Src-induced tyrosine phosphorylation of Cav-1 (*40*). Using sequence homology, we deduced a conserved tyrosine kinase recognition motif (QLFMADDSpY) centered at tyrosine 19 in the Cav-2 sequence. We have determined that c-Src can catalyze the phosphorylation of Cav-2 at tyrosine 19 (*41*). In an attempt to identify upstream mediators for this phenomenon, we have shown that signaling through the insulin receptor in adipocytes, as well as integrin ligation of endothelial cells, induced the phosphorylation of Cav-2 at tyrosine 19 (*41*).

One known function for tyrosine phosphorylation is to confer docking sites for Src-homology domain 2 (SH2)-containing proteins. Ligand stimulation induces tyrosine phosphorylation of the receptor itself and/or of accessory proteins. Numerous downstream signaling molecules are then recruited to the cytoplasmic face of the plasma membrane and utilize their SH2 domains to bind tyrosine-phosphorylated proteins. In this way, SH2 domain-containing proteins act as effectors in the transmission of signals. We have previously shown that tyrosine-phosphorylated Cav-1 directly interacts with the SH2 domain-containing molecule, Grb7 (*40*), and that phosphorylation of Cav-2 at tyrosine 19 induces the binding of three SH2 domain-containing proteins, including c-Src, Nck, and Ras-GAP (*41*).

Besides the tyrosine kinase recognition motif centered at tyrosine 19, Cav-2 contains a conserved motif for recognition by SH2 domain-containing proteins (pYADP) centered at tyrosine 27. In this study, we have attempted to evaluate whether Cav-2 is tyrosine-phosphorylated at residue 27. To this end, we generated a phospho-specific monoclonal antibody that specifically recognizes Cav-2 only when phosphorylated at tyrosine 27. Here, we show that Cav-2 is dually phosphorylated at both tyrosines 19 and 27. Also, we show that either c-Src expression or EGF stimulation is sufficient to induce these tyrosine phosphorylation events. We discuss the possible implications of the dual tyrosine phosphorylation of Cav-2 in a cellular context.

EXPERIMENTAL PROCEDURES

Materials. The full-length cDNA encoding human Cav-2 (residues 1−162) was subcloned into pCB7, a mammalian expression vector driven by the cytomegalovirus (CMV) promoter, as previously described (*11, 25*). C-terminally Myc-tagged cDNAs encoding human Cav-2 mutants were generated by PCR mutagenesis using mutated oligonucleotides, essentially as previously described (*41*), and subcloned into pCB7. The cDNA encoding human wild-type (WT) c-Src in the pUSEamp cytomegalovirus-based vector was purchased from Upstate Biotechnology, Inc. NIH 3T3 cells stably expressing c-Src were generously provided by Drs. Shalloway and Dehn (Cornell University, Ithaca, NY). Antibodies used in this study were obtained from the following vendors: anti-Cav-2 IgG (mAb 65) and anti-phosphotyrosine IgG (mAb PY20) from BD Pharmingen, anti-Myc IgG (mouse mAb 9E10 and rabbit pAb) from Santa Cruz Biotechnology, Inc., and anti-Cav-2 pAb from Affinity Bioreagents. A431 cells were obtained from ATCC (Manassas, VA). Other reagents were purchased commercially: human EGF (Upstate Biotechnology, Inc.), donor calf serum (JRH Biosciences), fetal bovine serum (Invitrogen), prestained protein markers (Invitrogen), and Slow-Fade anti-fade reagent (Molecular Probes).

Anti-Phospho Cav-2 (pY27) Antibody Production. A monoclonal antibody directed against phospho-Cav-2 (pY27) was generated by immunizing mice with a synthetic tyrosine-phosphorylated peptide based on the human Cav-2 sequence [HSGLE(pY)ADPEK]. Mice showing the highest titer of immunoreactivity in RSV-transformed cells were used to create fusions with myeloma cells using standard protocols. Positive hybridomas were cloned twice by limiting dilution and injected into mice to produce ascites fluid. Clone #40 IgGs were purified by affinity chromatography on protein A−Sepharose. A polyclonal antibody to phospho-Cav-2 (pY19) was described previously (*41*) (Affinity Bioreagents).

Cell Culture. NIH 3T3 cells were grown in Dulbecco's modified Eagle's medium supplemented with glutamine, antibiotics (penicillin and streptomycin), and 10% donor calf serum (*42*). Cos-7 cells and A431 cells were grown in Dulbecco's modified Eagle's medium supplemented with glutamine, antibiotics (penicillin and streptomycin), and 10% fetal calf serum.

Transient Expression in Cos-7 Cells. cDNAs encoding C-terminally Myc-tagged human Cav-2 WT and mutants, including Y19A, Y27A, and Y19A/Y27A, were transiently transfected into Cos-7 cells alone or in combination with c-Src. Transfections were carried out using the Effectine transfection reagent (Qiagen), in accordance with the manufacturer's instructions. Thirty-six hours after transfection, cells were lysed in boiling SDS sample buffer and subjected to SDS−PAGE (12% acrylamide)/Western blot. Recombinant expression of Myc-tagged human Cav-2 was detected either with anti-Cav-2 IgG (mAb 65) recognizing full-length Cav-2 (*11*) or with mAb 9E10 recognizing the Myc epitope tag (EQKLISEEDLN).

Immunoprecipitation of WT Cav-2 and Mutants. Cos-7 cells were transiently transfected with cDNAs encoding either WT Cav-2 or Cav-2 mutants (Y19A, Y27A, and Y19A/Y27A), each alone or in combination with c-Src. Cells were harvested 36 h after transfection, and processed for immunoprecipitation with protein A−Sepharose CL-4B (Amersham Biosciences), as described previously (*41*). Briefly, cells were lysed in IP buffer containing 10 mM Tris (pH 8.0), 150 mM NaCl, 1% Triton X-100, and 60 mM octyl glucoside, supplemented with phosphatase and protease inhibitors. After preclearing had been carried out, lysates were immunoprecipitated using an anti-Myc rabbit polyclonal antibody. Finally, immunoprecipitates were washed five times with IP buffer, and resuspended in sample buffer. Samples were analyzed by SDS−PAGE, followed by Western blot analysis with a well-characterized monoclonal antibody against phosphotyrosine (PY20; BD Pharmingen).

Immunoblotting with Anti-Phospho Cav-2 Antibodies. Cells were lysed in boiling sample buffer. Samples were then boiled for 5 min, followed by a brief sonication. Cellular proteins were resolved by SDS−PAGE (12% acrylamide) and transferred to nitrocellulose membranes (Schleicher and Schuell, 0.2 μm). Blots were blocked for 2 h in TBST [10 mM Tris-HCl (pH 8.0), 150 mM NaCl, and 0.2% Tween 20] containing 5% bovine serum albumin (BSA). Then, the nitrocellulose membranes were incubated for 2 h with primary antibodies [either anti-phospho-Cav-2 (pY19) pAb diluted 500-fold or anti-phospho-Cav-2 (pY27) mAb diluted 500-fold] in a 1% BSA/TBST solution. Membranes were then washed with TBST, and incubated for 1 h with the appropriate horseradish peroxidase-conjugated secondary antibody (diluted 5000-fold in a 1% BSA/TBST solution). IgG binding was visualized with an ECL detection kit (Pierce). Peptide competition assays were performed, as previously described (*41*). Briefly, each competitor peptide was premixed with the primary antibody solution at a concentration of 100 μg/mL (~100-fold molar excess of peptide) prior to Western blotting.

Establishment of NIH 3T3 Cell Lines Stably Expressing Human Cav-2. Parental NIH 3T3 cells and NIH 3T3 cells expressing c-Src were transfected with Myc-tagged human WT Cav-2 using lipofectamine reagent (Invitrogen) in accordance with the manufacturer's instructions. Hygromycin B (200 μg/mL) resistant clones were individually isolated using cloning rings. Lysates were prepared, and c-Myc expression was analyzed by SDS−PAGE/Western blotting. Clones expressing human Cav-2 were cultured in the presence of selection medium for four to six passages. The resistant cells were then cultured in the absence of an antibiotic for four additional passages, before proceeding with further experiments.

Immunofluorescence. All steps for immunofluorescence were carried out at room temperature. NIH 3T3 cells stably expressing human WT Cav-2 and c-Src were grown on coverslips. Then, cells were washed with PBS and fixed for 30 min in PBS containing 2% paraformaldehyde. After fixation, cells were briefly rinsed with PBS, and permeabilized with 0.1% Triton X-100 for 10 min. Cells were then incubated for 10 min with a 50 mM NH_4Cl/PBS solution to quench free aldehyde groups. Cells were then incubated with primary antibodies for 60 min in PBS containing 0.2% BSA. We made three sets of primary antibody mixtures: (1) anti-phospho-Cav-2 (pY19) pAb and anti-phospho-Cav-2 (pY27) mAb, (2) anti-phospho-Cav-2 (pY27) mAb and anti-Cav-2 pAb, and (3) anti-phospho-Cav-2 (pY19) pAb and anti-Cav-2 mAb. Cells were then washed three times with PBS (10 min each) and incubated for 30 min with a mixture of lissamine rhodamine B sulfonyl chloride-conjugated goat anti-mouse antibody (5 μg/mL) and a fluorescein isothiocyanate-conjugated donkey anti-rabbit antibody (5 μg/mL) in PBS containing 0.2% BSA. Cells were washed three times with PBS (10 min each) and mounted on slides with Slow-Fade anti-fade reagent (Molecular Probes). After EGF stimulation, A431 cells were prepared for immunofluorescence in a similar fashion.

CCD Imaging and Deconvolution. Images were captured using an Olympus IX80 microscope equipped with a 60× Plan Neofluar objective and a Photometrics cooled CCD camera with a 35 mm shutter. Images were processed using the IP Lab program on a Power Mac 8500. Six to eight two-dimensional images were acquired for each stained sample. These images were then deconvoluted and combined to create one final image per sample.

Preparation of Caveolae-Enriched Membrane Fractions. NIH 3T3 cells stably expressing human Cav-2 and c-Src were lysed in 2 mL of ice-cold MES-buffered saline [MBS, 25 mM MES (pH 6.5) and 0.15 M NaCl] containing 1% (v/v) Triton X-100 (*32*, *43*−*47*). Cells were homogenized using 10 strokes in a Dounce homogenizer. Two milliliters of homogenate was mixed with 2 mL of a 80% sucrose solution, prepared in MBS, to yield a final concentration of 40% sucrose, and placed at the bottom of an ultracentrifuge tube. A 5%/30% discontinuous sucrose gradient was layered on top of the homogenate. Samples were spun at 39 000 rpm for 16 h in an SW 41 rotor (Beckman Instruments). A light scattering band confined to the 5−30% interface was observed that contained Cav-1, but excluded most other cellular proteins. Twelve fractions (1 mL) were collected from the top of each gradient. Equal amounts from each fraction were separated by SDS−PAGE and subjected to Western blot analysis.

Velocity Gradient Centrifugation. NIH 3T3 cells stably coexpressing human Cav-2 and c-Src were lysed in MBS containing 60 mM octyl glucoside. Samples were loaded atop a 5 to 40% linear sucrose gradient and centrifuged at 50 000 rpm for 10 h in an SW 60 rotor (*11*, *12*, *22*, *25*). Fractions were collected from the top of each gradient and analyzed by SDS−PAGE/Western blotting. Molecular mass standards for velocity gradient centrifugation were as we described previously (*11*, *12*, *22*, *25*).

Stimulation of A431 Cells with EGF. A431 human epithelial cells were incubated overnight in serum-free media. Cells were then incubated with EGF (at a final concentration of 100 nM), for increasing periods of time at 37 °C. Then, cells were subjected either to SDS−PAGE/Western blotting or to immunofluorescence analysis.

Tyrosine-Phosphorylated GST−Cav-2 Proteins. GST−Cav-2 fusion proteins (in the pGEX-4T-1 vector) were generated by PCR-assisted subloning, using the human Cav-2 cDNAs as a template, essentially as we described previously (*48*). The following constructs were generated: GST−Cav-2 WT, GST−Cav-2 Y19A, GST−Cav-2 Y27A, GST−Cav-2 Y19A/Y27A. All four constructs contained the complete N-terminal domain of human caveolin-2 (residues 1−86). GST constructs were transformed into two different *Escherichia coli* strains, to generate either tyrosine-phosphorylated or nonphosphorylated GST fusion proteins. Transformation of the constructs into the BL21 (DE3) strain yielded a nonphosphorylated GST−Cav-2 fusion protein, whereas transformation of the constructs into the TKB1 strain yielded a tyrosine-phosphorylated GST−Cav-2 protein. The TKB1 strain is a derivative of BL21 which harbors a plasmid-encoded isopropyl 1-thio-β-D-galactopyranoside (IPTG)-inducible tyrosine kinase gene (the Elk receptor tyrosine kinase domain, Stratagene, Inc.).

Detection of SH2 Domain-Containing Proteins that Bind Tyrosine-Phosphorylated Cav-2. Nonphosphorylated and tyrosine-phosphorylated GST−Cav-2 fusion proteins were purified, immobilized on glutathione−agarose beads, and incubated with NIH 3T3 cell lysates. These lysates were prepared in IP buffer containing a mixture of protease and phosphatase inhibitors [10 mM Tris (pH 8.0), 150 mM NaCl, 1% Triton X-100, 60 mM octyl glucoside, 50 mM NaF, 30 mM sodium pyrophosphate, 100 μM sodium orthovanadate, pepstatin A (1 μg/mL), and 1 tablet of complete protease inhibitor mixture (Roche Molecular Biochemicals)]. Following overnight incubation at 4 °C, agarose beads were washed extensively with lysis buffer, subjected to SDS−PAGE, and transferred to nitrocellulose membranes. Bound proteins were visualized by immunoblotting with a panel of antibodies directed against known SH2 domain-containing proteins (see Table 2 of ref *41*). These antibodies were purchased from BD Pharmingen.

RESULTS

Cav-2 Is Phosphorylated at Tyrosines 19 and 27 in Vivo. Analysis of its primary sequence reveals that Cav-2 contains a putative tyrosine kinase recognition motif at tyrosine 19, as well as an SH2 domain-binding motif at tyrosine 27. In a previous report, we were able to show that c-Src expression is sufficient to induce Cav-2 phosphorylation at tyrosine 19. However, it remains unknown whether Cav-2 is phosphorylated at tyrosine 27 as well. To investigate this issue, we generated three Myc-tagged variants of human WT Cav-2, with each consensus tyrosine mutated to alanine, either one at a time or in combination, i.e., Cav-2 Y19A, Cav-2 Y27A, and Cav-2 Y19A/Y27A. Cos-7 cells were then transfected with either WT Cav-2 or Cav-2 mutants in combination with c-Src. Cell lysates were prepared and immunoprecipitated using an anti-Myc rabbit polyclonal antibody. Cav-2 tyrosine phosphorylation was monitored by immunoblotting with a well-characterized mouse monoclonal antibody directed against anti-phosphotyrosine (PY20).

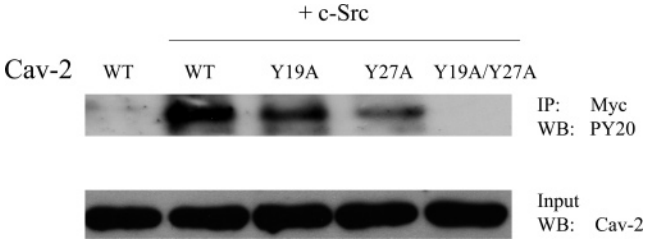

FIGURE 1: c-Src expression induces the phosphorylation of human Cav-2 on both tyrosine 19 and tyrosine 27 *in vivo*. To determine whether Cav-2 is phosphorylated at tyrosines 19 and 27, we generated Myc-tagged human Cav-2 mutants with tyrosine 19 and tyrosine 27 mutated to alanine, either singly or doubly, i.e., Cav-2 (Y19A), Cav-2 (Y27A), and Cav-2 (Y19A/Y27A). These constructs were then transfected into Cos-7 cells in combination with c-Src. Thirty-six hours post-transfection, cell lysates were subjected to immunoprecipitation using a rabbit polyclonal antibody directed against the C-terminal Myc epitope tag. Immunoprecipitates were then subjected to Western blot analysis with an antibody that recognizes phosphotyrosine (mouse mAb PY20). Note that c-Src expression is sufficient to induce the tyrosine phosphorylation of WT Cav-2. However, mutation of either tyrosine 19 or tyrosine 27 to alanine individually does not completely abrogate the phosphorylation of human Cav-2. Mutation of tyrosine 27, impeding phosphorylation at this site, strongly reduces the intensity of the signal, suggesting that tyrosine 27 may constitute the main phosphorylation site of Cav-2. Interestingly, the double mutation of Cav-2, i.e., Cav-2 (Y19A/Y27A), no longer demonstrates any reactivity toward the phosphotyrosine antibody PY20. Immunoblotting with the Cav-2 antibody is shown to demonstrate equal Cav-2 expression in the lysates prior to immunoprecipitation (input). Taken together, these results suggest that human Cav-2 is phosphorylated at tyrosines 19 and 27.

Figure 1 shows that WT Cav-2 is tyrosine-phosphorylated only in the presence of c-Src. Interestingly, coexpression of c-Src with either Cav-2 single mutant, Cav-2 Y19A or Cav-2 Y27A, diminished, but did not abolish, the tyrosine phosphorylation of Cav-2. These results suggest that although both tyrosines are indeed phosphorylated, neither one is the unique site for phosphorylation. However, coexpression of c-Src with the double mutant, in which both tyrosine sites were changed to alanine (Cav-2 Y19A/Y27A), totally abolishes Cav-2 tyrosine phosphorylation. These results suggest that Cav-2 is phosphorylated at tyrosine 19, as well as at tyrosine 27, and identify c-Src as one of the kinases responsible for this phosphorylation event.

Generation of a Phospho-Specific Antibody Directed against Cav-2 (pY27). To better characterize Cav-2 tyrosine phosphorylation, we generated a novel phospho-specific monoclonal antibody directed against Cav-2 (pY27) (clone #40). For this purpose, a tyrosine-phosphorylated human Cav-2 synthetic peptide [HSGLE(pY)ADPEK, residues 22−32] was used to immunize mice. We have previously generated and described a polyclonal antibody recognizing Cav-2 phosphorylated at tyrosine 19 (*41*). To determine the selectivity of anti-phospho-Cav-2 (pY27), Cos-7 cells were transiently transfected either with human WT Cav-2 or with Cav-2 mutants in the presence of c-Src.

Figure 2 shows that both anti-phospho-specific antibodies, anti-phospho-Cav-2 (pY19) and anti-phospho-Cav-2 (pY27), recognize WT Cav-2 only when coexpressed with c-Src. However, when tyrosine 27 is mutated to alanine, preventing

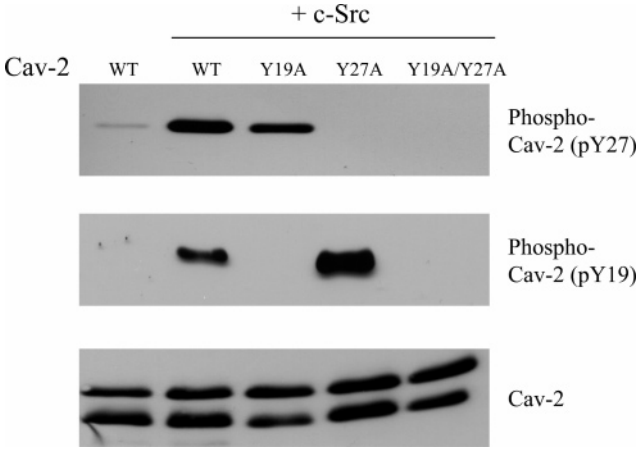

FIGURE 2: Characterization of a newly generated monoclonal antibody specific for phospho-Cav-2 (pY27) (mAb clone #40). A synthetic human Cav-2 peptide phosphorylated on tyrosine 27 was used to immunize mice and generate a phospho-specific probe directed against phospho-Cav-2 (pY27). We have previously generated a phospho-specific antibody against Cav-2 (pY19) (*41*). Cos-7 cells were transiently transfected with cDNAs encoding human WT Cav-2 or Cav-2 mutants, alone or in combination with c-Src. Note that both phospho-specific antibodies, anti-phospho-Cav-2 (pY19) and anti-phospho-Cav-2 (pY27), recognize WT Cav-2 only in the presence of c-Src, strongly supporting the idea that Cav-2 is phosphorylated at tyrosines 19 and 27. Mutation at either tyrosine 19 or tyrosine 27 to alanine abolishes the reactivity of the phospho-specific antibody raised against a given residue, Cav-2 (pY19) or Cav-2 (pY27), respectively. These results demonstrate that the anti-phospho-Cav-2 (pY27) antibody is specific solely for tyrosine-phosphorylated Cav-2 at position 27, and confirms that our anti-phospho-Cav-2 (pY19) antibody is specific solely for tyrosine-phosphorylated Cav-2 at position 19. Western blot analysis with an anti-Cav-2 antibody is shown as a control for equal protein loading.

A

Name	Sequence
Cav-2 (Y19)	MDDDSYSHHSGL
Cav-2 (pY19)	MDDDS(pY)SHHSGL
Cav-2 (Y27)	HSGLEYADPEK
Cav-2 (pY27)	HSGLE(pY)ADPEK

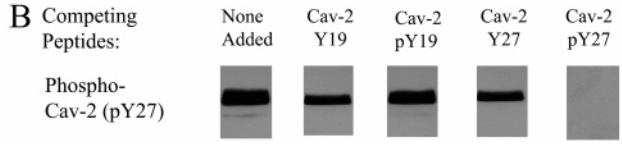

FIGURE 3: Anti-phospho-Cav-2 (pY27) antibody maintains its specificity when challenged with peptides structurally related to the immunogen. To examine the specificity of anti-phospho-Cav-2 (pY27) IgG, we performed a competition assay using various synthetic peptides derived from human Cav-2 phosphorylation motifs: Cav-2 (Y19), Cav-2 (pY19), Cav-2 (Y27), and Cav-2 (pY27). (A) Sequences of the peptides that were employed. (B) Cos-7 cells were cotransfected with human WT Cav-2 and c-Src. Thirty-six hours after transfection, cells were lysed in boiling sample buffer, subjected to SDS−PAGE, and transferred to nitrocellulose. The nitrocellulose was then cut into strips and incubated with anti-phospho-Cav-2 (pY27) IgG, alone or in combination with the aforementioned peptides. Note that both unphosphorylated Cav-2 peptides, i.e., Cav-2 (Y19) and Cav-2 (Y27), and the tyrosine-phosphorylated Cav-2 peptide (pY19) have no effect on the reactivity of the anti-phospho-Cav-2 (pY27) antibody. However, immunoreactivity was completely abolished when the immunogen, Cav-2 (pY27), was incubated along with the antibody.

phosphorylation at this site, the immunoreactivity of the anti-phospho-Cav-2 (pY27) antibody was completely abolished. Conversely, the anti-phospho-Cav-2 (pY19) antibody failed to recognize the Cav-2 (Y19A) mutant coexpressed with c-Src. Interestingly, the double mutant Cav-2 (Y19A/Y27A) retained no immunoreactivity toward either antibody. These results demonstrate that both phospho-specific Cav-2 antibodies, anti-phospho-Cav-2 (pY19) and anti-phospho-Cav-2 (pY27), confer exclusive detection of their respective phosphotyrosine residues.

The specificity of the anti-phospho-Cav-2 (pY27) antibody was further analyzed by performing a competition assay using synthetic peptides derived from the human Cav-2 sequence. Figure 3A shows the sequences of the unphosphorylated and phosphorylated versions of the peptides employed, i.e., Cav-2 (Y19) and Cav-2 (pY19), centered at tyrosine 19, and Cav-2 (Y27) and Cav-2 (pY27), centered at tyrosine 27. Lysates from Cos-7 cells transiently cotransfected with c-Src and human Cav-2 cDNAs were subjected to Western blot analysis using anti-phospho-Cav-2 (pY27) IgG, alone or in combination with one of the above-mentioned peptides. Figure 3B shows that only the immunogen, the Cav-2 (pY27) peptide, was able to block the immunoreactivity of the anti-phospho-Cav-2 (pY27) antibody. The unphosphorylated version of the same peptide, Cav-2 (Y27), as well as Cav-2 (pY19), in which the phosphotyrosine is located only eight amino acids downstream from the critical residue, had no effect on antibody immunoreactivity. These studies clearly demonstrate the selectivity of this novel monoclonal antibody (clone #40) in detecting phospho-Cav-2 (pY27).

Phosphorylation of Cav-2 at Tyrosines 19 and 27 Is Induced by c-Src in Stably Transfected NIH 3T3 Cells. We next asked whether Cav-2 tyrosine phosphorylation is cell type-specific or is a more general phenomenon. To this end, we generated NIH 3T3 cells stably expressing Myc-tagged human WT Cav-2, in the presence or absence of c-Src. Recombinant expression of Myc-tagged Cav-2 was monitored by Western blotting with Cav-2 or c-Myc antibodies (Figure 4). Note that the Cav-2 antibody recognizes an upper band that corresponds to the recombinant Myc-tagged Cav-2, as well as a lower band that corresponds to the endogenous protein. Cav-2 phosphorylation was monitored by immunoblotting with anti-phospho-Cav-2 (pY19) and anti-phospho-Cav-2 (pY27) antibodies. Interestingly, we could detect Cav-2 phosphorylation at both tyrosine 19 and tyrosine 27 only in NIH 3T3 cells stably coexpressing human Cav-2 and c-Src. In a manner similar to that of the previous experiments using transiently transfected Cos-7 cells, phosphorylation of Cav-2 at tyrosines 19 and 27 was strictly dependent on the expression of c-Src. Interestingly, the phospho-Cav-2 (pY19) antibody also detected the phosphorylation of endogenous Cav-2 in NIH 3T3 cells expressing c-Src, suggesting that the Cav-2 (pY19) antibody also recognizes the mouse Cav-2 protein sequence. Since it was generated by immunizing mice with a human-derived Cav-2 peptide, the anti-phospho-Cav-2 (pY27) antibody does not cross-react with the endogenous mouse protein.

Cav-2 Phosphorylated at Tyrosine 19 or Tyrosine 27 Displays Distinct Subcellular Localization. To gain new insight into the functional significance of the two tyrosine-

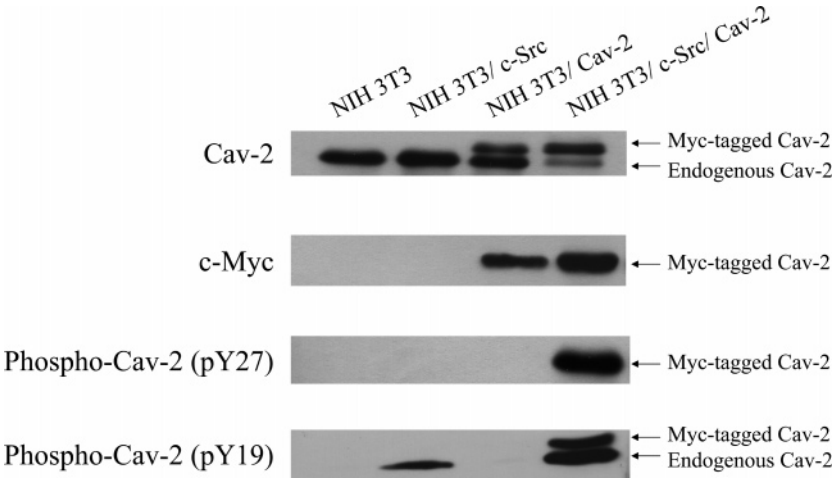

FIGURE 4: Cav-2 is phosphorylated at tyrosines 19 and 27 in NIH 3T3 cells. NIH 3T3 cells stably expressing Myc-tagged human WT Cav-2 and c-Src were generated. Expression of stably transfected Myc-tagged human Cav-2 was monitored with anti-Cav-2 IgG. Note that, in the top panel, the upper bands correspond to recombinant Myc-tagged human Cav-2 (lanes 3 and 4), whereas the lower bands represent endogenous murine Cav-2 (see arrows). Immunoblotting with the anti-Myc antibody demonstrates that recombinant Cav-2 is strongly expressed in the transfected NIH 3T3 cells (second panel, lanes 3 and 4). The phosphorylation state of Cav-2 at tyrosines 19 and 27 was monitored with anti-phospho-Cav-2 (pY19) and anti-phospho-Cav-2 (pY27) antibodies (third and fourth panels, respectively). Note that both phospho-specific antibodies recognize recombinant Cav-2 only in the presence of c-Src. In addition, the anti-phospho-Cav-2 (pY19) antibody detects the endogenous murine Cav-2 phosphorylated at tyrosine 19 (fourth panel, lanes 2 and 4, lower bands). Since the phospho-Cav-2 (pY27) antibody was generated using the human peptide, it does not cross-react with the mouse sequence.

phosphorylated forms of Cav-2, we next determined their respective subcellular localization patterns. We reasoned that if phospho-Cav-2 (pY19) and phospho-Cav-2 (pY27) had different localization patterns, they might exert distinct functions in the cell. To this end, we doubly immunostained NIH 3T3 cells stably expressing c-Src and human Cav-2 with different combinations of anti-phospho-Cav-2 (pY19), anti-phospho-Cav-2 (pY27), and anti-Cav-2 antibodies.

As shown in Figure 5A, double labeling with the anti-phospho-Cav-2 (pY19) polyclonal antibody and the anti-phospho-Cav-2 (pY27) monoclonal probe revealed two distinct localization patterns for the two different phosphorylated forms of Cav-2. Phospho-Cav-2 (pY19) was localized mainly along the periphery of the cell, predominantly concentrated in areas of cell−cell contact, while phospho-Cav-2 (pY27) was distributed in a dotlike pattern on the cell membrane and in an intracellular region of the cell. Figure 5D shows a merged color image to better illustrate the different localization patterns. Furthermore, double labeling with the anti-phospho-Cav-2 (pY19) polyclonal antibody and the anti-Cav-2 monoclonal antibody revealed that total Cav-2 and phospho-Cav-2 (pY19) do not colocalize (Figure 5B). Similarly, immunostaining with the anti-phospho-Cav-2 (pY27) monoclonal probe in combination with the anti-Cav-2 polyclonal antibody showed that the subcellular distribution of phospho-Cav-2 (pY27) does not coincide with the pattern observed for total Cav-2 (Figure 5C). Taken together, these results suggest that the two tyrosine-phosphorylated forms of Cav-2 are concentrated in different regions within the same cell, and that only a subpopulation of Cav-2 is phosphorylated at tyrosine 19 or tyrosine 27. However, it is important to note that we were able to detect some Cav-2 immunostaining at areas of cell−cell contacts, and in intracellular dots in overexposed images with the Cav-2 antibodies (data not shown).

Upon c-Src-Induced Phosphorylation of Tyrosines 19 and 27, Cav-2 Remains Associated with Lipid Rafts but Is Unable to Form High-Molecular Mass Hetero-Oligomeric Complexes. To further evaluate the phenotypic behavior of phospho-Cav-2 (pY19) and phospho-Cav-2 (pY27), we investigated their biochemical properties. At the level of the endoplasmic reticulum, Cav-1 and -2 directly interact with each other to form a high-molecular mass hetero-oligomeric complex, which contains ~14−16 individual caveolin molecules (*22*). As they reach the Golgi level, these ~300−350 kDa hetero-oligomeric units are incorporated into membrane microdomains, called lipid rafts (*43*). Lipid rafts are characterized by a special lipid composition, particularly enriched in cholesterol and sphingolipids (*49*). During their progression through the Golgi complex, these hetero-oligomeric units self-associate via their carboxy termini and drive the formation of a caveolae-sized vesicle, which is ultimately targeted to the plasma membrane (*29*). The unusual lipid composition of lipid rafts and caveolae confers special biochemical properties upon these microdomains, namely, a reduced buoyant density as compared to their phospholipid counterparts, and resistance to solubilization by nonionic detergents, such as Triton X-100, at low temperatures. These characteristics constitute the basis for the purification and isolation of lipid rafts and caveolae. Cav-1 is able to form a stable homo-oligomeric complex associated with the inner face of the cell membrane. Phosphorylation of Cav-1 at tyrosine 14 does not affect its oligomerization ability or caveolar targeting (*40*). Cav-2, on the other hand, is unable to form homo-oligomers and requires association with Cav-1 to exit the Golgi complex and to be targeted to the plasma membrane (*30*, *31*).

We first attempted to evaluate whether Cav-2 phosphorylation at tyrosine 19 and 27 would affect its caveolar targeting. To purify lipid rafts and/or caveolin-enriched membranes, we employed a well-established sucrose gradient ultracentrifugation method using NIH 3T3 cells stably transfected with c-Src and human Cav-2. Figure 6A shows that Cav-2 migrates in fractions 4−6, which are the lipid

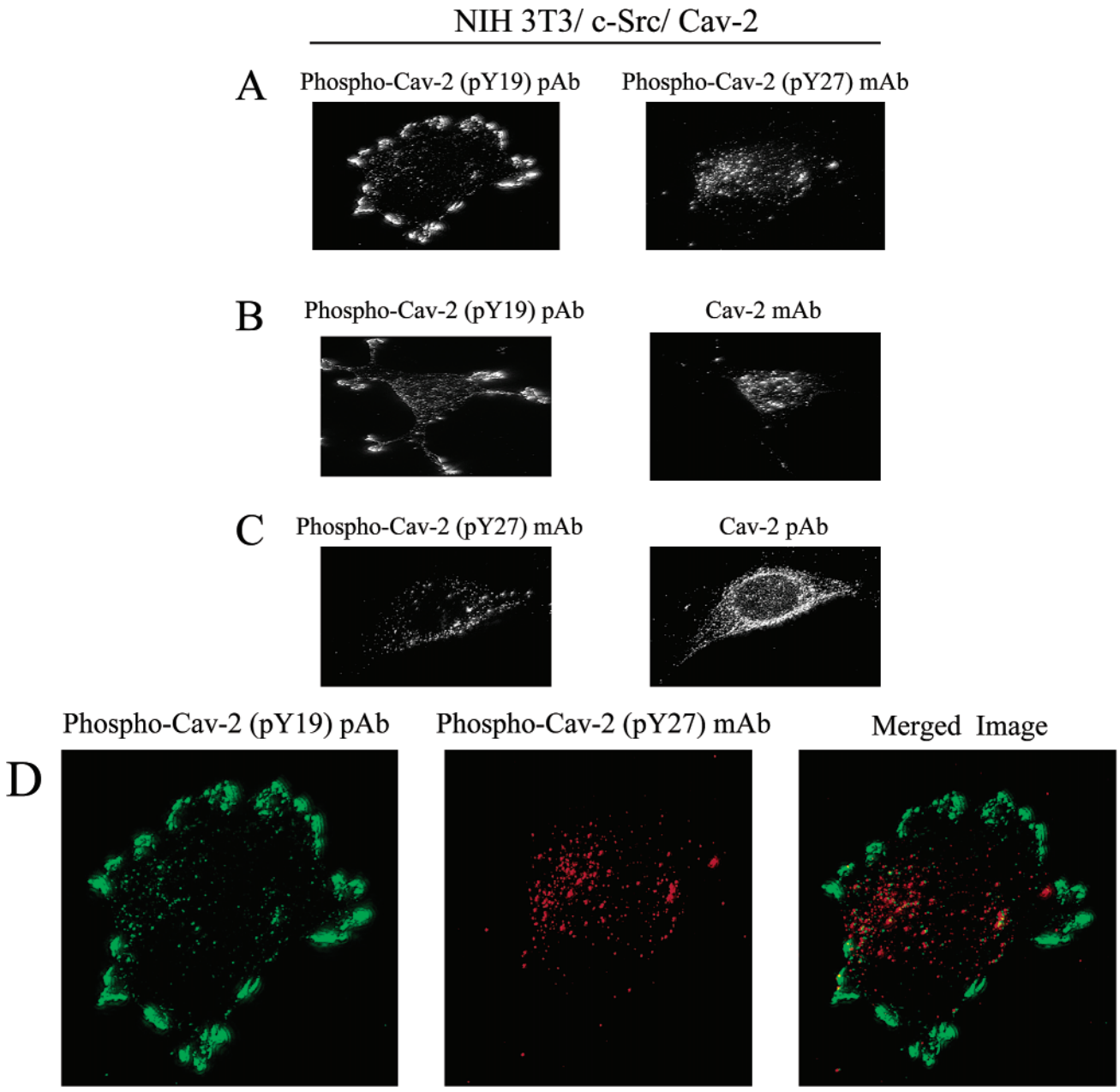

FIGURE 5: Distinct localization of phospho-Cav-2 (pY19) and phospho-Cav-2 (pY27), within the same cell. NIH 3T3 cells stably expressing human Cav-2 and c-Src were doubly immunostained with different combinations of Cav-2 antibodies. The bound primary antibodies were then visualized using distinctly tagged fluorescent secondary antibodies. Images were acquired with an Olympus IX80 microscope connected to a cooled CCD camera. (A) Anti-phospho-Cav-2 (pY19) pAb and anti-phospho-Cav-2 (pY27) mAb. Note that phospho-Cav-2 (pY19) appears to be enriched at the cell periphery, at cell−cell contacts (left panel). Staining with anti-phospho-Cav-2 (pY27) generated a dotted pattern intracellularly and on the cell surface (right panel). These results indicate that phospho-Cav-2 (pY19) and phospho-Cav-2 (pY27) have different localization patterns within the same cell, and that different molecules of Cav-2 are phosphorylated either at tyrosine 19 or at tyrosine 27. (B) Anti-phospho-Cav-2 (pY19) pAb and anti-Cav-2 mAb. Note that phospho-Cav-2 (pY19) (left panel) and total Cav-2 (right panel) have different localization patterns, suggesting that the majority of Cav-2 is not localized in the proximity of the major sites of Cav-2 phosphorylation on tyrosine 19 *in vivo*. (C) Anti-phospho-Cav-2 (pY27) mAb and anti-Cav-2 pAb. Note that the phospho-Cav-2 (pY27) localization pattern does not completely coincide with the distribution of total Cav-2, suggesting that only a fraction of Cav-2 is phosphorylated at tyrosine 27. (D) Merged image. Color versions of the images in panel A are shown along with the merged image to better illustrate the distinct localization of phospho-Cav-2 (pY19) and phospho-Cav-2 (pY27), within the same cell.

rafts and/or caveolae-enriched membrane fractions. Interestingly, tyrosine phosphorylation at residues 19 and 27 did not affect the association of Cav-2 with lipid rafts or caveolae.

Next, we evaluated the oligomerization state of tyrosine-phosphorylated Cav-2 by performing velocity gradient ultracentrifugation on NIH 3T3 cells stably transfected with c-Src and human Cav-2. Figure 6B shows that Cav-2 is able to form hetero-oligomers with Cav-1 of ~350−440 kDa, clearly showing that Cav-2 behaves as expected in our cellular system. However, phospho-Cav-2 (pY19) migrates as a monomer/dimer (<66 kDa), and is unable to form a high-molecular mass complex, whereas phospho-Cav-2 (pY27) is present as a monomer (~29 kDa). Taken as a whole, these results illustrate that neither phospho-Cav-2 (pY19) nor phospho-Cav-2 (pY27) is able to properly

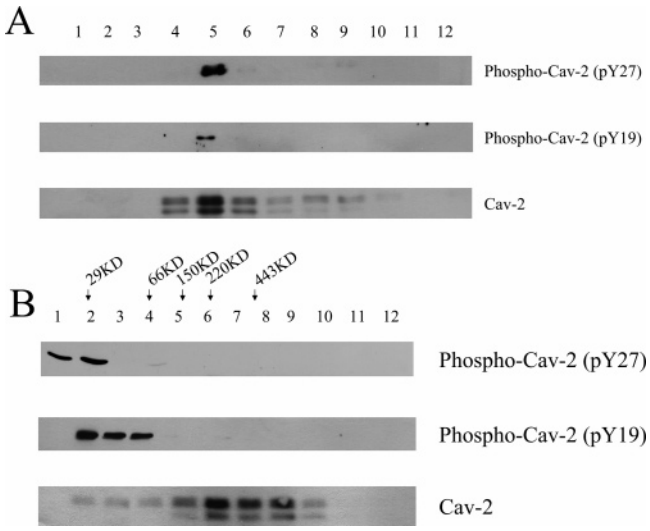

FIGURE 6: Tyrosine phosphorylation impedes Cav-2 hetero-oligomerization but allows it to remain associated with lipid rafts and/or caveolae. In both panels, tyrosine-phosphorylated Cav-2 was detected with anti-phospho-Cav-2 (pY19) and anti-phospho-Cav-2 (pY27) antibodies. Total Cav-2 was visualized using mAb 65. (A) Caveolar targeting. NIH 3T3 cells stably expressing c-Src and human WT Cav-2 were homogenized in a buffer containing 1% Triton X-100 and subjected to sucrose density gradient ultracentrifugation. Twelve fractions (1 mL) were collected, and the same amounts from each fraction were analyzed by Western blotting. Note that Cav-2 is enriched in fractions 4 and 5, which represent the lipid raft/caveolae−membrane fractions. Note that phospho-Cav-2 (pY19) and phospho-Cav-2 (pY27) are targeted to the lipid raft/caveolae−membrane fractions, in a fashion similar to that of total Cav-2. (B) Velocity gradient analysis. NIH 3T3 cells stably expressing c-Src and human Cav-2 WT were solubilized, placed atop a 5 to 40% sucrose density gradient, and ultracentrifuged for 10 h. Twelve fractions were collected, and a 50 μL aliquot from each fraction was analyzed by SDS−PAGE followed by Western blotting. The molecular mass standards are indicated above. Note that phospho-Cav-2 (pY19) behaved as monomer/dimer ($<$66 kDa), while phospho-Cav-2 (pY27) is found as a monomer ($\leq$29 kDa). In contrast, total Cav-2 migrated as a high-molecular mass hetero-oligomer ($>$150 kDa).

oligomerize, but each continues to be targeted to caveolae membranes. Consistent with these results, we have previously shown that phospho-Cav-2 (pY19) remains confined to lipid rafts, but it is no longer able to associate with high-molecular mass Cav-1 oligomers (*41*).

EGF Stimulation Induces the Phosphorylation of Endogenous Cav-2 on both Tyrosine 19 and Tyrosine 27 in Human A431 Cells. To evaluate the upstream signals that might induce Cav-2 tyrosine phosphorylation, we used A431 cells, a human epidermal carcinoma-derived cell line, which endogenously coexpresses the epidermal growth factor (EGF) receptor, Cav-1, and Cav-2. In a previous study, we have shown that addition of EGF is sufficient to stimulate the phosphorylation of Cav-1 on tyrosine 14 in this cell type (*40*). A431 cells were first serum starved overnight, and then treated with EGF for various periods of time. Phosphorylation was monitored by immunoblotting with anti-phospho-Cav-2 (pY19) and anti-phospho-Cav-2 (pY27) antibodies.

Brief treatment (5 min) of A431 cells with EGF induced Cav-2 phosphorylation at tyrosines 19 and 27 (Figure 7). However, while phosphorylation on tyrosine 27 was sustained or slightly increased with time, phosphorylation on tyrosine 19 reached maximal levels at 5 min and then

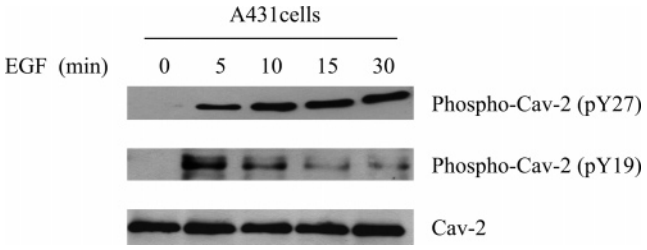

FIGURE 7: EGF stimulation induces the phosphorylation of endogenous Cav-2 at tyrosines 19 and 27 in human A431 cells. After overnight serum starvation, human epidermal A431 cells were treated with 100 ng/mL EGF for different time periods. Cells were then lysed and analyzed by Western blotting with anti-phospho-Cav-2 (pY19) and anti-phospho-Cav-2 (pY27) antibodies. Note that within 5 min, EGF stimulation induces the phosphorylation of endogenous Cav-2 at both tyrosine residues. However, the levels of phospho-Cav-2 (pY19) reach a maximal peak at 5 min and then decline; on the other hand, phospho-Cav-2 (pY27) appears at 5 min and then its level slightly increases (~2-fold) with time. Equal loading was assessed by Western blotting with an anti-Cav-2 antibody that recognizes total caveolin-2.

declined. These results suggest that phosphorylation of Cav-2 at tyrosine 19 or 27 may play different roles or may represent a switching point for the signaling response to EGF. Alternatively, tyrosine phosphorylation of Cav-2 at tyrosine 19 may precede the phosphorylation at tyrosine 27 in this EGF-induced signal transduction pathway.

To directly visualize the localization of each phosphorylated form of endogenous Cav-2, we immunostained A431 cells with phospho-specific anti-Cav-2 antibodies, in the presence or absence of EGF. Figure 8A shows that upon EGF stimulation, phospho-Cav-2 (pY19) accumulated at the plasma membrane, and its concentration was highest in areas of cell−cell contact. In the same cell, phospho-Cav-2 (pY27) appeared to be scattered at the cell surface and intracellularly. Figure 8D shows a merged picture of these images, to better demonstrate the distinct localization patterns of phospho-Cav-2 (pY19) and phospho-Cav-2 (pY27), within the same cells. Importantly, these localization patterns we observed in the endogenous system closely resembled those we described in NIH 3T3 recombinantly expressing human Cav-2 (see Figure 5 for comparison).

We next asked whether in EGF-stimulated A431 cells, phospho-Cav-2 (pY19) or phospho-Cav-2 (pY27) had a pattern similar or overlapping with that of total Cav-2. Panels B and C of Figure 8 show that both phospho-Cav-2 (pY19) and phospho-Cav-2 (pY27) had quite distinct localization patterns as compared to total Cav-2, suggesting that endogenously only a subpopulation of Cav-2 is tyrosine-phosphorylated. However, Cav-2 immunostaining can be detected to some extent at areas of cell−cell contact and in intracellular dots in overexposed images (data not shown). Importantly, we did not observe any immunostaining with the anti-phospho-Cav-2 (pY19) or anti-phospho-Cav-2 (pY27) antibodies using unstimulated A431 cells (data not shown).

As EGF stimulation induces phosphorylation of Cav-2 at tyrosines 19 and 27 in a different temporal fashion, we next evaluated whether the distribution patterns of phospho-Cav-2 (pY19) and phospho-Cav-2 (pY27) would change with time in response to EGF. For this purpose, A431 cells were EGF-stimulated for increasing amounts of time (5, 15, 30, 60, and 120 min), and then doubly immunostained with anti-phospho-Cav-2 (pY19) or anti-phospho-Cav-2 (pY27) an-

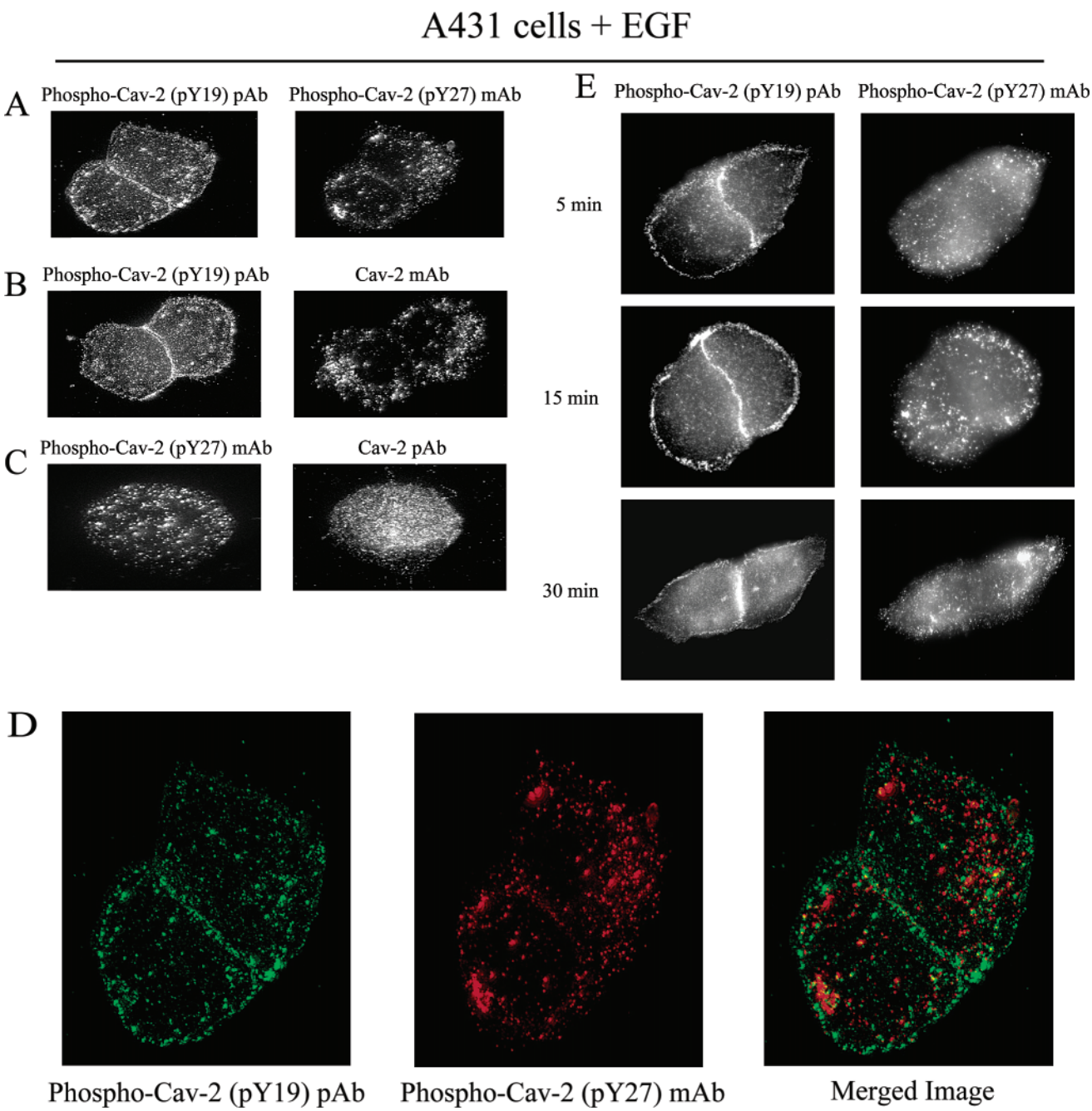

FIGURE 8: Independent segregation of tyrosine-phosphorylated forms of endogenous Cav-2 in response to EGF stimulation of A431 cells. A431 cells were serum starved overnight and then treated with 100 ng/mL EGF for 20 min (A−D) or for increasing periods of time (E). Cells were then fixed and doubly labeled with a variety of antibodies, as detailed below. (A) Anti-phospho-Cav-2 (pY19) pAb and anti-phospho-Cav-2 (pY27) mAb. Phospho-Cav-2 (pY19) was concentrated at the plasma membrane, in the areas of cell−cell contact. Phospho-Cav-2 (pY27) exhibits a patchy pattern that is distributed intracellularly and over the cell surface. (B) Anti-phospho-Cav-2 (pY19) pAb and anti-Cav-2 mAb. Note that the cellular distributions of phospho-Cav-2 (pY19) and total Cav-2 do not coincide, suggesting that only a fraction of Cav-2 is phosphorylated at tyrosine 19. (C) Anti-phospho-Cav-2 (pY27) mAb and anti-Cav-2 pAb. Note the different localization patterns of phospho-Cav-2 (pY27) and total Cav-2. This suggests that only a subpopulation of Cav-2 is phosphorylated at tyrosine 27. (D) Merged image. Color versions of panel A are shown along with the merged image to better illustrate the independent segregation of phospho-Cav-2 (pY19) and phospho-Cav-2 (pY27). (E) Anti-phospho-Cav-2 (pY19) pAb and anti-phospho-Cav-2 (pY27) mAb. A431 cells were stimulated with EGF for different periods of time. At 5, 15, and 30 min, phospho-Cav-2 (pY19) was localized at the plasma membrane, in the areas of cell−cell contact. At the same time points, phospho-Cav-2 (pY27) displays a dotlike pattern that is distributed intracellularly and over the cell surface. These results suggest that, at different times of EGF stimulation, the cellular distribution of phospho-Cav-2 (pY19) and of phospho-Cav-2 (pY27) does not significantly change. Virtually identical results were obtained at 60 and 120 min (data not shown).

tibodies. Figure 8E shows that, over this period of time, phospho-Cav-2 (pY19) is consistently concentrated at areas of cell−cell contact, while phospho-Cav-2 (pY27) is consistently found in a dotlike pattern. These results suggest that phospho-Cav-2 (pY19) and phospho-Cav-2 (pY27) are not found in the same cellular regions at any time point, and that the distribution of the two molecules does not significantly change in response to short or longer EGF stimulation. However, the intensity of staining and the overall numbers of cells which were stained with anti-phospho-Cav-2

(pY19) antibody decreased with time, while anti-phospho-Cav-2 (pY27) staining became stronger with time from 5 to 15 min, with the appearance of larger and brighter dots. However, from 15 to 120 min, the immunostaining signal from phospho-Cav-2 (pY27) remained relatively constant.

Taken together, these results demonstrate that in A431 cells, EGF stimulation induces the phosphorylation of endogenous Cav-2 at tyrosines 19 and 27. However, upon EGF stimulation, phospho-Cav-2 (pY19) and phospho-Cav-2 (pY27) display different kinetic responses and distinct subcellular distributions, suggesting that phosphorylation of Cav-2 at tyrosine 19 or 27 may play different roles in EGF-induced signaling, and may not occur within the same time frame.

Tyrosine-Phosphorylated Cav-2 Binds to SH2 Domain-Containing Proteins, Ras-GAP, c-Src, and Nck. To further dissect the pathways in which phospho-Cav-2 (pY19) and phospho-Cav-2 (pY27) are involved, we next attempted to identify their downstream mediators. We reasoned that phosphorylation of Cav-2 at tyrosine 19 or 27 could activate different partners or, alternatively, could bind the same molecules with different affinity, thereby indicating that the two sites may play different functional roles in cell physiology. Phosphotyrosine often serves as a binding site for SH2 domain-containing proteins. To determine whether any SH2 domain-containing proteins would bind Cav-2, we generated a variety of constructs containing either WT Cav-2 or Cav-2 mutants fused to GST, i.e., GST−WT Cav-2, GST−Cav-2 (Y19A), GST−Cav-2 (Y27A), and GST−Cav-2 (Y19A/Y27A). GST fusion proteins were then purified from two different bacterial strains, to yield either unphosphorylated proteins (from the BL21 strain) or tyrosine-phosphorylated proteins (from the TKB1 stain).

First, we attempted to evaluate the phosphorylation pattern of the GST−Cav-2 fusion proteins purified from the TKB1 strain. Equal amounts of proteins were subjected to SDS−PAGE, followed by Western blotting with antibodies against anti-phospho-Cav-2 (pY19), anti-phospho-Cav-2 (pY27), and Cav-2. Figure 9A shows that GST−WT Cav-2 is phosphorylated at tyrosines 19 and 27. However, GST−Cav-2 (Y19A) is still phosphorylated at tyrosine 27, but not at residue 19, while GST−Cav-2 (Y27A) is still phosphorylated at tyrosine 19, but not at residue 27. Importantly, GST−Cav-2 (Y19A/27A) is no longer phosphorylated at tyrosines 19 and 27. These results suggest that ablation of one tyrosine phosphorylation site does not interfere with phosphorylation on the other site, and suggests that the two phosphorylation events can occur independently.

We evaluated the binding partners of these GST−Cav-2 fusion proteins, by incubating them with lysates from normal NIH 3T3 cells. After extensive washing, the proteins were subjected to SDS−PAGE. Bound proteins were identified by immunoblotting with a panel of antibodies directed against SH2 domain-containing proteins (see Table 2 of ref *41*). Figure 9B shows that, out of the 21 antibodies tested, only three proteins, Ras-GAP, c-Src, and Nck, were found to interact with GST−WT Cav-2. It is important to note that the binding was strictly dependent on tyrosine phosphorylation of Cav-2. Importantly, no binding was observed with GST alone.

We next examined whether there were any differences in protein binding affinity or selectivity between the two phosphotyrosine residues, i.e., phospho-Cav-2 (pY19) and phospho-Cav-2 (pY27). Figure 9B demonstrates that both Cav-2 single mutants, i.e., GST−Cav-2 (Y19A) and GST−Cav-2 (Y27A), still retain some ability to bind Ras-GAP, c-Src, and Nck, indicating a role for both of these residues

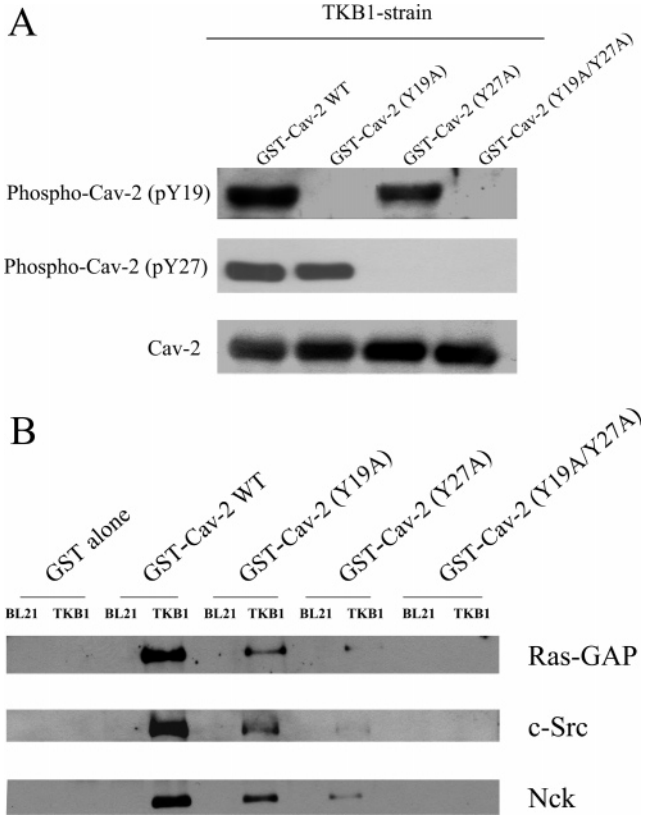

FIGURE 9: Phosphorylation of Cav-2 at tyrosine 27 is critical for binding to three SH2 domain-containing proteins: Ras-GAP, c-Src, and Nck. GST fusion proteins containing human WT Cav-2 and human Cav-2 mutants (Y19A, Y27A, and Y19A/Y27A) were purified from two bacterial strains. Purification from the BL21 strain yields unphosphorylated proteins. In contrast, purification from the TKB1 strain, which harbors a tyrosine kinase, generates tyrosine-phosphorylated proteins. (A) GST−Cav-2 fusion proteins purified from the TKB1 strain were subjected to Western blot analysis with antibodies directed against anti-phospho-Cav-2 (pY19), anti-phospho-Cav-2 (pY27), and anti-Cav-2. Note that GST−Cav-2 (Y19A) is still phosphorylated at tyrosine 27, but not at residue 19, while GST−Cav-2 (Y27A) is phosphorylated at tyrosine 19, but not at tyrosine 27. However, GST−Cav-2 (Y19A/Y27A) is no longer phosphorylated at tyrosine 19 and 27. Equal loading was assessed by immunoblotting with the Cav-2 antibody. (B) Fusion proteins were incubated with cell lysates derived from NIH 3T3 cells. Bound materials were identified with a panel of antibodies directed against SH2 domain-containing proteins. Note that of the 21 proteins surveyed, only three, Ras-GAP, c-Src, and Nck, bind Cav-2 in a phospho-dependent fashion. These three SH2 domain-containing proteins retained some ability to bind Cav-2 when either critical tyrosine residue was singly mutated to alanine, i.e., GST−Cav-2 (Y19A) or GST−Cav-2 (Y27A). However, mutation of tyrosine 19 to alanine decreased the amount of binding proteins compared to the amount of WT Cav-2. Furthermore, the GST−Cav-2 (Y27A) mutant exhibited significantly less binding than the GST−Cav-2 (Y19A) mutant. Finally, no binding was detected with a double mutant in which both phosphorylation sites are ablated, i.e., GST−Cav-2 (Y19A/Y27A). Importantly, no binding to unphosphorylated GST−Cav-2 or GST alone was observed. Taken together, these results provide evidence that binding of Cav-2 to Ras-GAP, c-Src, and Nck is strictly dependent on tyrosine phosphorylation, and suggest that phosphorylation of Cav-2 at residue 27 is the most critical for binding to occur.

in the recruitment of SH2 domain-containing proteins. However, the amount of proteins that bound to the tyrosine-phosphorylated GST−Cav-2 (Y19A) was significantly smaller than the amount that bound to tyrosine-phosphorylated GST−WT Cav-2. Moreover, GST−Cav-2 (Y27A), which is still phosphorylated at tyrosine 19, but not at tyrosine 27, retained very little binding to Ras-GAP, c-Src, and Nck, as compared to GST−WT Cav-2 and GST−Cav-2 (Y19A). These results suggest that phosphorylation at tyrosine 27 is the most critical for the binding of the three SH2 domain-containing proteins, and indicates that phospho-Cav-2 (pY19) and phospho-Cav-2 (pY27) display differential binding of these SH2 domain-containing proteins. Consequently, we may speculate that phospho-Cav-2 (pY19) and phospho-Cav-2 (pY27) may play different roles in signal transduction. Importantly, disruption of both consensus tyrosines in GST−Cav-2 (Y19A/Y27A) resulted in the complete abrogation of binding to these three SH2 domain-containing proteins. Consistent with these results, we have previously determined that three such proteins, Ras-GAP, c-Src, and Nck, have the ability to associate with phospho-Cav-2 (pY19) (*41*).

DISCUSSION

In this study, we present new evidence demonstrating that Cav-2 undergoes phosphorylation at both tyrosines 19 and 27. We were able to detect these phosphorylation events in Cos-7 and NIH 3T3 cells recombinantly expressing human Cav-2 and c-Src, as well as in an endogenous setting using EGF-stimulated human A431 cells.

To monitor the tyrosine phosphorylation of Cav-2, we generated and extensively characterized a novel mouse monoclonal antibody probe that is specific for phospho-Cav-2 (pY27). We had previously generated a phospho-specific rabbit polyclonal antibody against Cav-2 (pY19) (*41*) and showed that Cav-2 is phosphorylated at tyrosine 19 (*41*). For the generation of a monoclonal antibody specific for phospho-Cav-2 (pY27), we immunized mice by injecting a synthetic peptide based on the human sequence. As the murine and human sequences are quite divergent around tyrosine 27, the phospho-Cav-2 (pY27) antibody does not recognize the mouse protein. For this reason, we carried out all of our experiments either by recombinant expression of the human Cav-2 protein or by evaluating the endogenous tyrosine phosphorylation of Cav-2 in human cells.

We first reconstituted these phosphorylation events by recombinant coexpression of c-Src and human Cav-2 in Cos-7 cells. Western blot analysis using anti-phospho-Cav-2 (pY19) and anti-phospho-Cav-2 (pY27) antibodies clearly shows that Cav-2 undergoes phosphorylation at tyrosines 19 and 27. Importantly, Cav-2 tyrosine phosphorylation is strictly dependent on the expression of c-Src. Interestingly, mutation of either of these two tyrosines to alanine inhibits, but does not abrogate, the phosphorylation of Cav-2, suggesting that neither of them is the unique phosphorylation site. In support of this view, double mutation of tyrosines 19 and 27 to alanine completely abolished the tyrosine phosphorylation of human Cav-2.

Experiments using NIH 3T3 cells stably expressing c-Src and human Cav-2 further illustrate that Cav-2 undergoes phosphorylation at both tyrosine 19 and tyrosine 27, corroborating the idea that c-Src induces these phosphorylation events to occur. Immunofluorescence analysis of NIH 3T3 cells stably transfected with c-Src and human Cav-2 allowed us to visualize the dual tyrosine phosphorylation of Cav-2. Phospho-Cav-2 (pY19) was predominantly enriched at regions of cell−cell contact, whereas phospho-Cav-2 (pY27) revealed a speckled pattern of staining, both at the plasma membrane and in the cytoplasm. Consistent with these results, we have previously shown that phospho-Cav-1 (pY14) and phospho-Cav-2 (pY19) colocalize in the proximity of focal adhesions (*40*, *41*). As phospho-Cav-2 (pY19) and phospho-Cav-2 (pY27) display such different subcellular localization patterns within the same cell, we speculate that they may play different functional roles.

Next, we examined the biochemical properties of the two phosphorylated forms of Cav-2. Both phospho-Cav-2 (pY19) and phospho-Cav-2 (pY27) continue to be targeted to lipid rafts, but are no longer able to form high-molecular mass oligomers. However, the two forms of phosphorylated human Cav-2 behaved differently in velocity gradients, with phospho-Cav-2 (pY19) acting as a monomer/dimer, and phospho-Cav-2 (pY27) behaving as a monomer.

To identify upstream mediators of the tyrosine phosphorylation of Cav-2, we monitored this event in an endogenous setting, by EGF stimulation of human A431 cells. Here, we show that Cav-2 undergoes phosphorylation at tyrosines 19 and 27 in response to signaling through the EGF receptor. However, EGF stimulation induces phosphorylation of Cav-2 at tyrosine 19 and at tyrosine 27 in a different fashion. First, the response to the EGF stimulus evolves within a different time frame. In fact, we show that Cav-2 undergoes rapid and transient phosphorylation at tyrosine 19 within 5 min, whereas phosphorylation at tyrosine 27 occurs at 5 min and is steadily maintained over a 30 min time period. These results evoke the possibility that phosphorylation of Cav-2 at tyrosine 19 may temporarily precede phosphorylation at tyrosine 27. Second, immunofluorescence analysis revealed that, upon EGF stimulation, phospho-Cav-2 (pY19) and phospho-Cav-2 (pY27) display different localization patterns within the same cell, which is similar to what we observed in NIH 3T3 cells stably transfected with c-Src and human Cav-2.

To begin to understand the downstream signaling of tyrosine-phosphorylated Cav-2, we performed an *in vitro* binding assay using GST fusion proteins. In this way, we identified three SH2 domain-containing proteins, Ras-GAP, c-Src, and Nck, which specifically associate with tyrosine-phosphorylated Cav-2. However, phospho-Cav-2 (pY19) and phospho-Cav-2 (pY27) show different binding preferences toward the three SH2 domain-containing proteins. In fact, mutation of tyrosine 27 significantly inhibited the binding to SH2 domain-containing proteins, whereas mutation of tyrosine 19 did not exert an equally strong effect. These results suggest that phosphorylation at tyrosine 27 is more critical than phosphorylation at tyrosine 19 for binding to occur. Consistent with our previous studies, we identified the same SH2 domain-containing proteins, Ras-GAP, c-Src, and Nck, as binding partners for phospho-Cav-2 (pY19) (*41*).

It is well-known that growth factors and integrin stimulation activate the Ras-p42/44 MAP kinase pathway, and lead to cell cycle progression and cell proliferation. At cell edges, these stimuli assemble focal adhesion molecules, which activate signaling through FAK and other proteins. Several

pieces of evidence suggest that Cav-1 might play a role in this scenario. First, Cav-1 was shown to act as a linker between integrins and the tyrosine kinase Fyn (*50*). Upon activation, Fyn recruits Shc, which in turn associates with Grb2 and activates the Ras-p42/44 MAP kinase pathway (*50*). Second, we have previously found that integrin stimulation triggers the colocalization of phospho-Cav-1 (pY14) and phospho-Cav-2 (pY19) with activated FAK at regions of cellular contact (*40*, *41*). Third, we have previously shown that the interaction between the SH2 domain-containing protein Grb7 and phospho-Cav-1 (pY14) stimulates anchorage-independent growth and cell migration (*40*). Although it is possible that tyrosine phosphorylation of Cav-2 may also be involved in such processes, it must signal through alternate molecules as neither tyrosine 19 nor tyrosine 27 was found to bind to Grb7.

The results we present in this study begin to highlight the complex role that tyrosine-phosphorylated Cav-2 may play in the activation of the Ras-p42/44 MAP kinase pathway. The key elements in this scenario are the ability of phospho-Cav-2 to localize at focal adhesions and to bind Ras-GAP, a molecule which acts as an inhibitor of Ras signaling. Although phospho-Cav-2 (pY27) constitutes the critical binding partner for Ras-GAP, it does not concentrate at focal contacts but rather scatters diffusely throughout the cell. Conversely, phospho-Cav-2 (pY19) is distributed near cell edges, but weakly binds Ras-GAP. As such, we envision that tyrosine phosphorylation of Cav-2 may contribute in a dual fashion to the signaling from growth factors and integrin stimulation, regulating the activation of the Ras-p42/44 MAP kinase pathway. In fact, EGF stimulation of A431 cells suggests that phosphorylation of Cav-2 at tyrosine 19 may temporarily precede phosphorylation at tyrosine 27. First, in response to EGF, phospho-Cav-2 (pY19) may accumulate at the cell edges and then phospho-Cav-2 (pY27) might shift the binding of Ras-GAP away from focal contacts, thus participating in the regulation of the Ras-p42/44 MAP kinase pathway. These results imply that tyrosine phosphorylation of Cav-2 at residue 19 and at residue 27 may play different yet complementary roles in response to certain cellular cues.

REFERENCES

1. Palade, G. E. (1953) Fine Structure of Blood Capillaries, *J. Appl. Phys. 24*, 1424−1436.
2. Yamada, E. (1955) The fine structure of the gall bladder epithelium of the mouse, *J. Biophys. Biochem. Cytol. 1*, 445−458.
3. Couet, J., Li, S., Okamoto, T., Scherer, P. S., and Lisanti, M. P. (1997) Molecular and cellular biology of caveolae: Paradoxes and Plasticities, *Trends Cardiovasc. Med. 7*, 103−110.
4. Fielding, P. E., and Fielding, C. J. (1995) Plasma membrane caveolae mediate the efflux of cellular free cholesterol, *Biochemistry 34*, 14288−14292.
5. Lisanti, M. P., Scherer, P., Tang, Z.-L., and Sargiacomo, M. (1994) Caveolae, caveolin and caveolin-rich membrane domains: A signalling hypothesis, *Trends Cell Biol. 4*, 231−235.
6. Anderson, R. G., Kamen, B. A., Rothberg, K. G., and Lacey, S. W. (1992) Potocytosis: sequestration and transport of small molecules by caveolae, *Science 255* (5043), 410−411.
7. Smart, E. J., Ying, Y.-S., Donzell, W. C., and Anderson, R. G. W. (1996) A role for caveolin in transport of cholesterol from endoplasmic reticulum to plasma membrane, *J. Biol. Chem. 271*, 29427−29435.
8. Smart, E. J., Graf, G. A., McNiven, M. A., Sessa, W. C., Engelman, J. A., Scherer, P. E., Okamoto, T., and Lisanti, M. P. (1999) Caveolins, liquid-ordered domains, and signal transduction, *Mol. Cell. Biol. 19* (11), 7289−7304.
9. Glenney, J. R., Jr., and Soppet, D. (1992) Sequence and expression of caveolin, a protein component of caveolae plasma membrane domains phosphorylated on tyrosine in Rous sarcoma virus-transformed fibroblasts, *Proc. Natl. Acad. Sci. U.S.A. 89* (21), 10517−10521.
10. Engelman, J. A., Zhang, X. L., Galbiati, F., Volonte, D., Sotgia, F., Pestell, R. G., Minetti, C., Scherer, P. E., Okamoto, T., and Lisanti, M. P. (1998) Molecular Genetics of the Caveolin Gene Family: Implications for Human Cancers, Diabetes, Alzheimer's Disease, and Muscular Dystrophy, *Am. J. Hum. Genet. 63*, 1578−1587.
11. Scherer, P. E., Okamoto, T., Chun, M., Nishimoto, I., Lodish, H. F., and Lisanti, M. P. (1996) Identification, sequence and expression of caveolin-2 defines a caveolin gene family, *Proc. Natl. Acad. Sci. U.S.A. 93*, 131−135.
12. Tang, Z.-L., Scherer, P. E., Okamoto, T., Song, K., Chu, C., Kohtz, D. S., Nishimoto, I., Lodish, H. F., and Lisanti, M. P. (1996) Molecular cloning of caveolin-3, a novel member of the caveolin gene family expressed predominantly in muscle, *J. Biol. Chem. 271*, 2255−2261.
13. Song, K. S., Scherer, P. E., Tang, Z.-L., Okamoto, T., Li, S., Chafel, M., Chu, C., Kohtz, D. S., and Lisanti, M. P. (1996) Expression of caveolin-3 in skeletal, cardiac, and smooth muscle cells. Caveolin-3 is a component of the sarcolemma and co-fractionates with dystrophin and dystrophin-associated glycoproteins, *J. Biol. Chem. 271*, 15160−15165.
14. Way, M., and Parton, R. (1995) M-caveolin, a muscle-specific caveolin-related protein, *FEBS Lett. 376*, 108−112.
15. Li, S., Song, K. S., Koh, S. S., Kikuchi, A., and Lisanti, M. P. (1996) Baculovirus-based expression of mammalian caveolin in Sf21 insect cells. A model system for the biochemical and morphological study of caveolar biogenesis, *J. Biol. Chem. 271*, 28647−28654.
16. Razani, B., Woodman, S. E., and Lisanti, M. P. (2002) Caveolae: from cell biology to animal physiology, *Pharmacol. Rev. 54* (3), 431−467.
17. Razani, B., Engelman, J. A., Wang, X. B., Schubert, W., Zhang, X. L., Marks, C. B., Macaluso, F., Russell, R. G., Li, M., Pestell, R. G., Di Vizio, D., Hou, H., Jr., Kneitz, B., Lagaud, G., Christ, G. J., Edelmann, W., and Lisanti, M. P. (2001) Caveolin-1 null mice are viable but show evidence of hyperproliferative and vascular abnormalities, *J. Biol. Chem. 276* (41), 38121−38138.
18. Drab, M., Verkade, P., Elger, M., Kasper, M., Lohn, M., Lauterbach, B., Menne, J., Lindschau, C., Mende, F., Luft, F. C., Schedl, A., Haller, H., and Kurzchalia, T. V. (2001) Loss of Caveolae, Vascular Dysfunction, and Pulmonary Defects in Caveolin-1 Gene-Disrupted Mice, *Science 293* (5539), 2449−2452.
19. Galbiati, F., Engelman, J. A., Volonte, D., Zhang, X. L., Minetti, C., Li, M., Hou, H., Kneitz, B., Edelmann, W., and Lisanti, M. P. (2001) Caveolin-3 null mice show a loss of caveolae, changes in the microdomain distribution of the dystrophin-glycoprotein complex, and T-tubule abnormalities, *J. Biol. Chem. 19*, 19.
20. Razani, B., Wang, X. B., Engelman, J. A., Battista, M., Lagaud, G., Zhang, X. L., Kneitz, B., Hou, H., Jr., Christ, G. J., Edelmann, W., and Lisanti, M. P. (2002) Caveolin-2-deficient mice show evidence of severe pulmonary dysfunction without disruption of caveolae, *Mol. Cell. Biol. 22* (7), 2329−2344.
21. Sowa, G., Pypaert, M., Fulton, D., and Sessa, W. C. (2003) The phosphorylation of caveolin-2 on serine 23 and 36 modulates caveolin-1-dependent caveolae formation, *Proc. Natl. Acad. Sci. U.S.A. 100* (11), 6511−6516.
22. Sargiacomo, M., Scherer, P. E., Tang, Z.-L., Kubler, E., Song, K. S., Sanders, M. C., and Lisanti, M. P. (1995) Oligomeric structure of caveolin: Implications for caveolae membrane organization, *Proc. Natl. Acad. Sci. U.S.A. 92*, 9407−9411.
23. Murata, M., Peranen, J., Schreiner, R., Weiland, F., Kurzchalia, T., and Simons, K. (1995) VIP21/caveolin is a cholesterol-binding protein, *Proc. Natl. Acad. Sci. U.S.A. 92*, 10339−10343.
24. Monier, S., Parton, R. G., Vogel, F., Behlke, J., Henske, A., and Kurzchalia, T. (1995) VIP21-caveolin, a membrane protein constituent of the caveolar coat, oligomerizes in vivo and in vitro, *Mol. Biol. Cell 6*, 911−927.
25. Scherer, P. E., Lewis, R. Y., Volonte, D., Engelman, J. A., Galbiati, F., Couet, J., Kohtz, D. S., van Donselaar, E., Peters, P., and Lisanti, M. P. (1997) Cell-type and tissue-specific expression

of caveolin-2. Caveolins 1 and 2 co-localize and form a stable hetero-oligomeric complex *in vivo*, *J. Biol. Chem. 272*, 29337−29346.
26. Lisanti, M. P., Tang, Z.-L., and Sargiacomo, M. (1993) Caveolin forms a hetero-oligomeric protein complex that interacts with an apical GPI-linked protein: Implications for the biogenesis of caveolae, *J. Cell Biol. 123*, 595−604.
27. Galbiati, F., Razani, B., and Lisanti, M. P. (2001) Emerging themes in lipid rafts and caveolae, *Cell 106* (4), 403−411.
28. Schlegel, A., and Lisanti, M. P. (2000) A molecular dissection of caveolin-1 membrane attachment and oligomerization. Two separate regions of the caveolin-1 C-terminal domain mediate membrane binding and oligomer/oligomer interactions in vivo, *J. Biol. Chem. 275* (28), 21605−21617.
29. Song, K. S., Tang, Z.-L., Li, S., and Lisanti, M. P. (1997) Mutational analysis of the properties of caveolin-1. A novel role for the C-terminal domain in mediating homotypic caveolin-caveolin interactions, *J. Biol. Chem. 272*, 4398−4403.
30. Parolini, I., Sargiacomo, M., Galbiati, F., Rizzo, G., Grignani, F., Engelman, J. A., Okamoto, T., Ikezu, T., Scherer, P. E., Mora, R., Rodriguez-Boulan, E., Peschle, C., and Lisanti, M. P. (1999) Expression of caveolin-1 is required for the transport of caveolin-2 to the plasma membrane. Retention of caveolin-2 at the level of the Golgi complex, *J. Biol. Chem. 274* (36), 25718−25725.
31. Mora, R., Bonilha, V. L., Marmorstein, A., Scherer, P. E., Brown, D., Lisanti, M. P., and Rodriguez-Boulan, E. (1999) Caveolin-2 localizes to the Golgi complex but redistributes to plasma membrane, caveolae, and rafts when co-expressed with caveolin-1, *J. Biol. Chem. 274* (36), 25708−25717.
32. Lisanti, M. P., Scherer, P. E., Vidugiriene, J., Tang, Z.-L., Hermanoski-Vosatka, A., Tu, Y.-H., Cook, R. F., and Sargiacomo, M. (1994) Characterization of caveolin-rich membrane domains isolated from an endothelial-rich source: Implications for human disease, *J. Cell Biol. 126*, 111−126.
33. Li, S., Couet, J., and Lisanti, M. P. (1996) Src tyrosine kinases, Gα subunits and H-Ras share a common membrane-anchored scaffolding protein, Caveolin. Caveolin binding negatively regulates the auto-activation of Src tyrosine kinases, *J. Biol. Chem. 271*, 29182−29190.
34. Song, K. S., Li, S., Okamoto, T., Quilliam, L., Sargiacomo, M., and Lisanti, M. P. (1996) Copurification and direct interaction of Ras with caveolin, an integral membrane protein of caveolae microdomains. Detergent free purification of caveolae membranes, *J. Biol. Chem. 271*, 9690−9697.
35. Li, S., Okamoto, T., Chun, M., Sargiacomo, M., Casanova, J. E., Hansen, S. H., Nishimoto, I., and Lisanti, M. P. (1995) Evidence for a regulated interaction of hetero-trimeric G proteins with caveolin, *J. Biol. Chem. 270*, 15693−15701.
36. Feron, O., Belhhassen, L., Kobzik, L., Smith, T. W., Kelly, R. A., and Michel, T. (1996) Endothelial nitric oxide synthase targeting to caveolae. Specific interactions with caveolin isoforms in cardiac myocytes and endothelial cells, *J. Biol. Chem. 271*, 22810−22814.
37. Garcia-Cardena, G., Oh, P., Liu, J., Schnitzer, J. E., and Sessa, W. C. (1996) Targeting of nitric oxide synthase to endothelilal cell caveolae via palmitoylation: implications for caveolae localization, *Proc. Natl. Acad. Sci. U.S.A. 93*, 6448−6453.
38. Song, K. S., Sargiacomo, M., Galbiati, F., Parenti, M., and Lisanti, M. P. (1997) Targeting of a Gα subunit (Gi1α) and c-Src tyrosine kinase to caveolae membranes: Clarifying the role of N-myristoylation, *Cell. Mol. Biol. (Noisy-Le-Grand) 43*, 293−303.
39. Glenney, J. R., Jr. (1989) Tyrosine phosphorylation of a 22-kDa protein is correlated with transformation by Rous sarcoma virus, *J. Biol. Chem. 264* (34), 20163−20166.
40. Lee, H., Volonte, D., Galbiati, F., Iyengar, P., Lublin, D. M., Bregman, D. B., Wilson, M. T., Campos-Gonzalez, R., Bouzahzah, B., Pestell, R. G., Scherer, P. E., and Lisanti, M. P. (2000) Constitutive and growth factor-regulated phosphorylation of caveolin-1 occurs at the same site (Tyr-14) in vivo: identification of a c-Src/Cav-1/Grb7 signaling cassette, *Mol. Endocrinol. 14* (11), 1750−1775.
41. Lee, H., Park, D. S., Wang, X. B., Scherer, P. E., Schwartz, P. E., and Lisanti, M. P. (2002) Src-induced phosphorylation of caveolin-2 on tyrosine 19. Phospho-caveolin-2 (Tyr(P)19) is localized near focal adhesions, remains associated with lipid rafts/caveolae, but no longer forms a high molecular mass hetero-oligomer with caveolin-1, *J. Biol. Chem. 277* (37), 34556−34567.
42. Koleske, A. J., Baltimore, D., and Lisanti, M. P. (1995) Reduction of caveolin and caveolae in oncogenically transformed cells, *Proc. Natl. Acad. Sci. U.S.A. 92* (5), 1381−1385.
43. Sargiacomo, M., Sudol, M., Tang, Z.-L., and Lisanti, M. P. (1993) Signal transducing molecules and GPI-linked proteins form a caveolin-rich insoluble complex in MDCK cells, *J. Cell Biol. 122*, 789−807.
44. Sargiacomo, M., Scherer, P. E., Tang, Z.-L., Casanova, J. E., and Lisanti, M. P. (1994) In vitro phosphorylation of caveolin-rich membrane domains: Identification of an associated serine kinase activity as a casein kinase II-like enzyme, *Oncogene 9*, 2589−2595.
45. Smart, E., Ying, Y.-S., Conrad, P., and Anderson, R. G. W. (1994) Caveolin moves from caveolae to the Golgi apparatus in response to cholesterol oxidation, *J. Cell Biol. 127*, 1185−1197.
46. Corley-Mastick, C., Brady, M. J., and Saltiel, A. R. (1995) Insulin stimulates the tyrosine phosphorylation of caveolin, *J. Cell Biol. 129*, 1523−1531.
47. Scherer, P. E., Tang, Z.-L., Chun, M. C., Sargiacomo, M., Lodish, H. F., and Lisanti, M. P. (1995) Caveolin isoforms differ in their N-terminal protein sequence and subcellular distribution: Identification and epitope mapping of an isoform-specific monoclonal antibody probe, *J. Biol. Chem. 270*, 16395−16401.
48. Sotgia, F., Lee, H., Bedford, M., Petrucci, T., Sudol, M., and Lisanti, M. P. (2001) Tyrosine phosphorylation of β-dystroglycan at its WW domain binding motif, PPxY, recruits SH2 domain containing proteins, *Biochemistry 40* (48), 14585−14592.
49. Simons, K., and Ikonen, E. (1997) Functional rafts in cell membranes, *Nature 387*, 569−572.
50. Wary, K. K., Mariott, I. A., Zurzolo, C., and Giancotti, F. G. (1998) A requirement for caveolin-1 and associated kinase Fyn in integrin signaling and anchorage-dependent cell growth, *Cell 94*, 625−634.

BI049295+